

## Thermalization Time of Hot Photoexcited Holes in *p*-Type Germanium\*

P. Norton and H. Levinstein

*Department of Physics, Syracuse University, Syracuse, New York 13210*

(Received 20 September 1971)

The thermalization time of hot photoexcited holes in *p*-type germanium has been investigated. This was accomplished by studying the mobility and recombination properties in a series of copper-doped-germanium samples, in which the carrier lifetime was systematically varied. Recombination-center densities were varied over five orders of magnitude, so that the transition from a thermalized to a hot photocarrier distribution was observed as the carrier lifetime became shorter. The carrier lifetime was measured directly from the photoresponse signal decay, for several samples, to establish the recombination cross section. A theory, assuming energy loss via optical- and acoustic-phonon emission, correctly predicts the increase in the average photoexcited-carrier energy as the recombination-center density is increased.

### I. INTRODUCTION

Many experiments, as well as several practical devices, rely on the photoexcitation of excess carriers in semiconductors, either from impurity states, or directly across the energy gap. These carriers are often injected with energies many times larger than the thermal equilibrium energy, so that, at least initially, they can be considered "hot" carriers. In the absence of a large electric field, the injected carrier will lose energy until it is in thermal equilibrium with the lattice. This thermalization time can be relatively long, compared with the carrier lifetime, especially at low temperatures. In those cases where the carrier lifetime is shorter than the time required for the carrier to thermalize, the photoexcited-carrier distribution will be hot. Several papers have reported the properties of such distributions,<sup>1-6</sup> but in most cases it is difficult to compare experiment with theory when such a situation occurs. In order to compare theoretical predictions which are based on an assumed thermal distribution with experiments based on photoexcited carriers, it is necessary that the carriers spend nearly all of their lifetime in a thermalized state. The purpose of this present paper is to report the thermalization time for photoexcited holes in *p*-type germanium. The thermalization time was measured by systematically varying the carrier lifetime, so that the transition from a thermal to a hot distribution could be identified as the carrier lifetime decreased. At the transition, the thermalization time will be about equal to the carrier lifetime. A measurement of the carrier lifetime at the transition is then a good approximation of the thermalization time.

We choose to measure two properties of the photoexcited carriers which are quite sensitive to the carrier-energy distribution. The first of these

properties is the average carrier mobility. At the low temperatures at which our measurements were made, the mobility of the carriers is strongly influenced by the presence of ionized impurities. The ionized-impurity-scattering time depends on the carrier energy to the  $\frac{3}{2}$  power,<sup>7</sup> plus a slowly varying logarithmic factor, so that the carrier mobility is a sensitive measure of the carrier energy. The analysis of mobility for nonhydrogenic acceptors such as copper in germanium has been discussed in detail for the case of thermally generated carriers.<sup>8</sup> However, in treating the situation of photoexcited carriers, when the thermalization time is longer than the carrier lifetime, the distribution of carrier energies is unknown. In order to make a quantitative comparison between the mobility data and the calculated mobility, we have had to assume a distribution function. We chose a  $\delta$  function for simplicity. This is unrealistic but it is a convenient device to characterize the average carrier energy.<sup>9</sup> For a  $\delta$ -function distribution, the mobility is given by

$$\mu = (e/m^*)\tau(\epsilon) \quad (1)$$

and differs from the expression for a thermal distribution in that  $\tau$ , the scattering time, is not averaged over the distribution. We must still calculate  $\tau$  separately for each band, including acoustic-phonon, ionized-impurity- and neutral-impurity-scattering contributions. As with the analysis of thermally generated carriers, interband scattering was only included for acoustic-phonon scattering, following the approximations of Bir, Normantas, and Pikus.<sup>10</sup>

The second property of the photoexcited carriers which we chose to study was the temperature dependence of the carrier lifetime. Carrier lifetime in germanium under extrinsic illumination is governed by the capture (recombination) of free carriers at ionized-impurity centers.<sup>11</sup> The prob-

ability for capture at an impurity center is also a function of the average carrier energy. If the carriers are in thermal equilibrium with the lattice, the average carrier energy will be  $\frac{3}{2}kT$ . For carriers in thermal equilibrium with the lattice, the average lifetime will follow the corresponding change in capture probability as the temperature is varied. On the other hand, the average energy of a hot distribution will not vary directly with temperature. Therefore the carrier lifetime will not show as strong a temperature dependence for a distribution of hot carriers.

## II. EXPERIMENTAL DETAILS

The carrier lifetime was systematically varied in a series of copper-doped-germanium samples. This was done by varying the density of recombination centers, which for low temperatures and weak illumination is equal to the density of compensating donors  $N_d$ . Compensation densities ranged from  $4 \times 10^{10}$  to  $6 \times 10^{15}$   $\text{cm}^{-3}$ , and were determined by analysis of the carrier concentration and mobility as a function of temperature.<sup>8</sup> The photo-Hall effect was used to measure the mobility and carrier concentration as a function of temperature between 3 and 20 K. Carriers were excited with 300-K background radiation, from which all photon energies greater than 0.23 eV had been removed by the use of cooled InSb filters. This prevented double ionization of the copper centers by the light (the second ionization level is 0.32 eV)<sup>12</sup> as well as excitation into the split-off valence band.<sup>13</sup>

Experimental data were taken in a random-temperature sequence, to eliminate the possibility that a drift in the illumination intensity would imply a temperature dependence. It was found that only a slight drift of a few percent occurred in the course of a measurement. Since only about  $10^9$  or less carriers were excited per cubic centimeter, a high-input-impedance electrometer (Keithley model 310B) was used to measure the Hall voltage. Both the photo-Hall and Hall measurements were made on the same sample by changing the radiation shields. However, even when the sample was removed and remeasured after several months, the reproducibility was excellent. The electric field applied to the sample was kept very weak to prevent carrier heating due to the presence of the field. The magnetic field was chosen to satisfy the high-field limit so that the Hall mobility could be set equal to the drift mobility.<sup>14</sup>

The carrier lifetime was measured from the decay of a photoexcited-carrier population, when the lifetime was sufficiently long to permit measurement. For this measurement the carriers were excited with a  $\text{CO}_2$  laser, modulated by an external GaAs crystal.<sup>15</sup> The details of this measurement will be the subject of a future paper.

Copper-doped germanium was selected for this experiment over shallow acceptors and other deep acceptors for several reasons. It has an activation energy about four times larger than the shallow acceptors. As a consequence, with copper-doped germanium we have been able to study the temperature dependence of the photoexcited-carrier mobility and lifetime over a much wider range (3–20 K) than would have been possible with shallow group-III acceptors. Another benefit of the larger activation energy of copper acceptors is that the hot photocarriers cannot impact ionize neutral-copper centers as easily as shallow acceptors. This is because carriers with enough energy to impact ionize copper centers will lose energy very rapidly via optical-phonon emission. Shallow acceptors would not be shielded from impact ionization by the optical-phonon-emission process, since the optical-phonon energy is greater than the activation energy of shallow acceptors. Although other deep-acceptor levels, such as mercury, could have been used, it is often very difficult to remove trace amounts of copper from germanium. Compensated copper centers in mercury-doped germanium could act as traps and cause extraneous phenomena which we wanted to avoid. The residual concentration of shallow-acceptor impurities was apparently quite low in our copper-doped samples, as indicated by the analysis of mobility,<sup>8</sup> so that trapping by these levels was very likely unimportant.

## III. EXPERIMENTAL RESULTS

Photo-Hall data taken in the course of this work can be put into two categories. The first group of samples diffused at 800 °C with copper concentrations around  $1.5 \times 10^{16}$   $\text{cm}^{-3}$  all showed appreciable effects of impurity-hopping conduction<sup>16</sup> while the second group, having lower concentrations of copper impurities, did not show any evidence of impurity conduction. Figure 1 shows the temperature dependence of the mobility and carrier concentration of sample N5g, which did not show any evidence of impurity conduction. As can be seen, there is very little temperature dependence of the photo-carrier concentration. The mobility of the carriers excited with the 300-K background is clearly enhanced, as can be seen by the increase in mobility around 20 K for the photo-Hall case.

The interaction of impurity conduction can cause very unusual behavior of the photo-Hall coefficient. Figure 2 shows the inverse Hall coefficient of sample N5e with 300-K background illumination at various magnetic fields as a function of temperature. As can be seen, the Hall coefficient reverses direction twice. At 22 K this is caused by the usual impurity-conduction interaction with thermally generated carriers. As the temperature decreases, the density of thermally generated car-

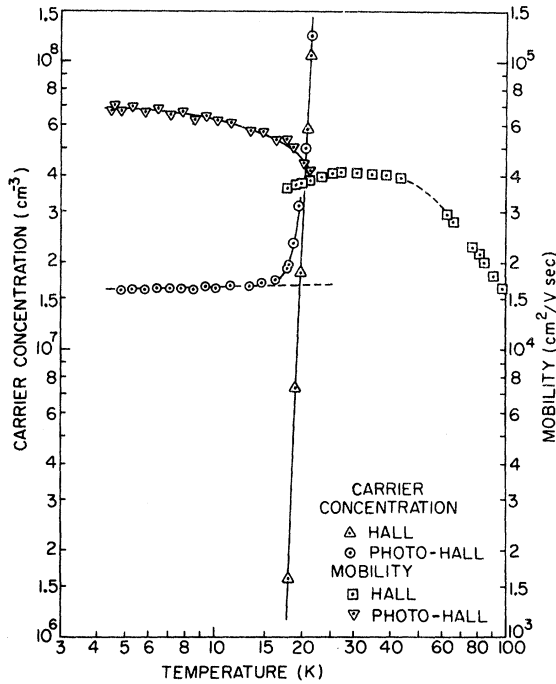


FIG. 1. Thermal and photoexcited carrier concentrations and mobility at low temperatures for copper-doped sample N5g. This sample did not show any impurity-hopping conduction.

riers continues to freeze out. Soon, however, the density of thermally excited carriers becomes negligible compared with those photoexcited. With the population of carriers thus stabilized, the Hall coefficient begins to level out, only to increase again as the impurity-conduction mechanism freezes out at still lower temperatures.<sup>17</sup> To analyze these data, one needs only to consider a very simple model. We define the conductivity due to impurity conduction as  $\sigma_i = e(n\mu)_i = 1/\rho_i$ .<sup>18</sup> This quantity can be measured directly, by measuring the sample resistance without illumination in the low-temperature region. From the behavior of such measurements between 10 and 15 K, it seems reasonable to extrapolate the conductivity due to the hopping process to higher temperatures in the vicinity of 20 K, since the hopping conduction in this region is relatively temperature independent. One more experimental result permits us to carry out a relatively direct analysis. The conductivity due to hopping has been found to show only a very weak magnetoresistance, with changes of less than 5% between zero and 20 kG.<sup>19</sup> Hence the impurity conduction can be viewed as a shorting resistance, its value depending only on temperature and not magnetic field. The appropriate result for the Hall coefficient is then given by

$$\mathcal{R} = \frac{(1/e)p\mu^2}{(p\mu + (n\mu)_i)^2 + (n\mu)_i^2 \mu^2 H^2}, \quad (2)$$

where  $p$  is the concentration of holes in the valence band, and  $\mu$  is their mobility. By restricting this equation to the high-field-limit region, the degeneracy of the valence band can be ignored. Measuring the Hall coefficient at two magnetic fields, and the resistivity, both with and without illumination, allows us to calculate  $\mu$  and  $p$ :

$$\mu = \frac{[p\mu + (n\mu)_i]^2}{(n\mu)_i^2} \frac{(\mathcal{R}_{H_1} - \mathcal{R}_{H_2})}{(\mathcal{R}_{H_2} H_2^2 - \mathcal{R}_{H_1} H_1^2)}, \quad (3)$$

$$p = (1/\mu^2) \mathcal{R}_{H_1} e \{ [p\mu + (n\mu)_i]^2 + (n\mu)_i^2 \mu^2 H^2 \}, \quad (4)$$

where

$$[p\mu + (n\mu)_i] = 1/e\rho_{11\text{ght}}, \quad (5)$$

$$(n\mu)_i = 1/e\rho_{\text{dark}}. \quad (6)$$

Using the above result, the carrier concentration and mobility of the photoexcited carriers were calculated for sample N5e. Measured resistivities and the Hall coefficient were taken from Fig. 2 for 4 and 8 kG. The result is given in Fig. 3. We now see the same characteristic behavior shown by sample N5g in Fig. 1.

Earlier measurements of photo-Hall data for copper-doped germanium neglected the effects of impurity conduction. Measurements on a copper-doped sample containing  $1.3 \times 10^{16}$ -cm<sup>-3</sup> copper and

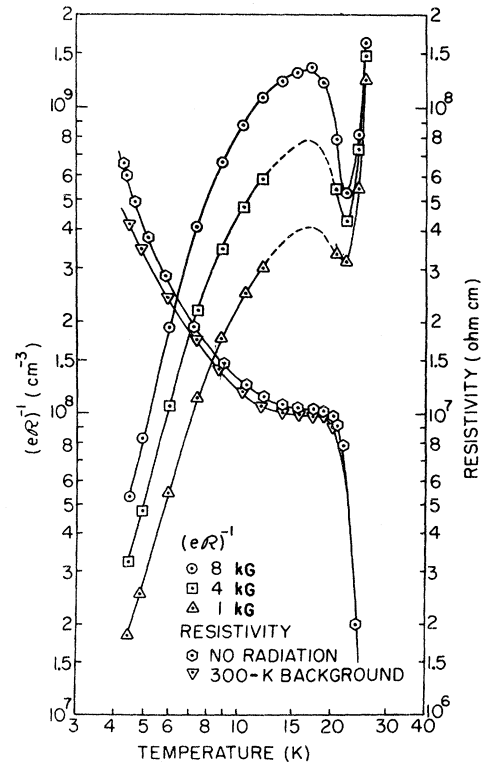


FIG. 2. Resistivity and inverse photo-Hall coefficient for sample N5e. This sample showed very strong impurity-hopping conduction.

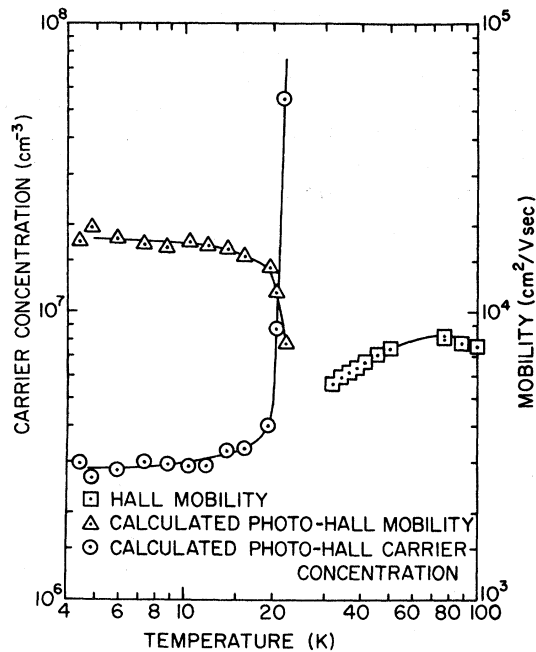


FIG. 3. Calculated photo-Hall carrier concentration and mobility using data shown in Fig. 2 for sample N5e.

about  $10^{15}$ - $\text{cm}^{-3}$  compensation were reported by Rollin and Rowell.<sup>1</sup> We felt that the bump in their curve of carrier concentration as a function of

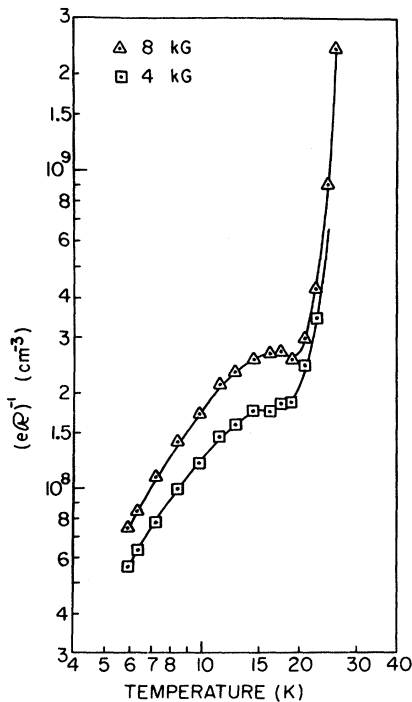


FIG. 4. Inverse photo-Hall coefficient for sample N5e with increased illumination (for comparison see Fig. 2).

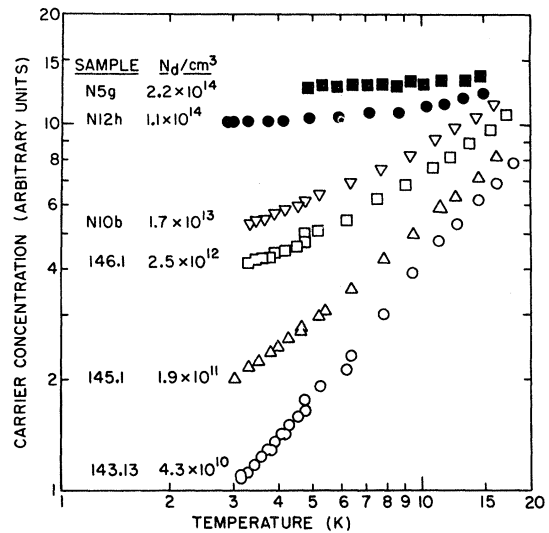


FIG. 5. Temperature dependence of the photocarrier concentration for six samples having different compensation densities. The vertical scale has been arbitrarily adjusted to facilitate comparison.

temperature near 15 K might have been caused by the same effect seen in Fig. 2. To check this, we remeasured sample N5e with increased illumination. A filtered Nernst glower was used to give about an order-of-magnitude increase in the photoexcited-carrier concentration. Figure 4 shows the results of this measurement at two magnetic field strengths. These curves are very similar to the curve published by Rollin and Rowell. Although we agree with the conclusion of these authors that the carrier distribution is hot, we will show later that the cross section does not have a  $T^{-4}$  dependence as they claim. An alternative explanation of the bump has been proposed by Barker and Hearn,<sup>20</sup> who suggest that it is due to a variation in the Hall factor, caused by a non-Boltzmann carrier distribution.

The influence of impurity conduction on the photo-Hall measurements was seen in samples with copper concentrations greater than  $10^{16}$   $\text{cm}^{-3}$ . Although we have demonstrated the possibility of extracting the photoexcited-carrier concentration and mobility in this case, we have preferred to use samples with no apparent impurity conduction for examining the temperature dependence of these quantities. This has been possible because the transition region sought in this experiment has been found in the range covered by samples having copper concentrations below  $10^{16}$   $\text{cm}^{-3}$ . As was seen in Figs. 1 and 3, the temperature dependences of samples N5g and N5e are identical once the effects of impurity conduction are taken into consideration. Therefore, no important change in the temperature dependence is seen to occur in the

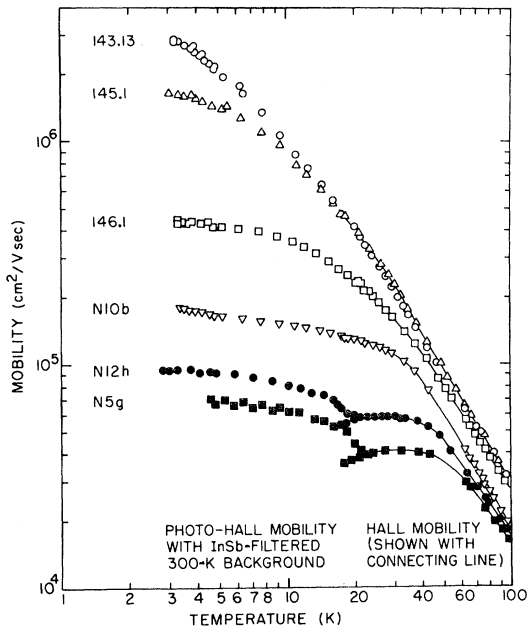


FIG. 6. Temperature dependence of the Hall and photo-Hall mobility for the six samples shown in Fig. 5.

range of donor concentrations between  $2 \times 10^{14}$  and  $6 \times 10^{15} \text{ cm}^{-3}$ .

The temperature dependence of the photocarrier concentration as a function of compensation is illustrated in Fig. 5. An arbitrary adjustment of the vertical scale was made to facilitate comparison. The change in the temperature dependence of the photocarrier concentration is seen to be considerable and systematic as  $N_d$  is varied from  $4.3 \times 10^{10}$  up to  $2.2 \times 10^{14} \text{ cm}^{-3}$ . The lowest donor concentration,  $4.3 \times 10^{10} \text{ cm}^{-3}$ , gives the strongest temperature dependence. This can be roughly approximated as proportional to  $T^{1.15}$ . Even in this region of very low compensation, there is a perceptible change of slope with compensation. We can see this by comparison with sample 145.1, having a donor concentration of  $1.9 \times 10^{11} \text{ cm}^{-3}$ . Below 10 K, sample 145.1 seems to show a slightly weaker temperature dependence than sample 143.13. The temperature dependence becomes weaker as we go up to a donor concentration of  $2.5 \times 10^{12} \text{ cm}^{-3}$ , as seen in sample 146.1. Very little change occurs as we increase the donor concentration to  $1.7 \times 10^{13} \text{ cm}^{-3}$ , evident in sample N10b. A dramatic shift to a virtually temperature-independent photocarrier concentration occurs as  $N_d$  is increased further. This is seen in samples N12h and N5g where the donor concentration is  $1.1 \times 10^{14}$  and  $2.2 \times 10^{14} \text{ cm}^{-3}$ , respectively. It is also observed in the calculated results of sample N5e shown in Fig. 3. The change to a temperature-independent carrier concentration is the result of

nonthermalization of the photoexcited carriers.

There were significant changes in the mobility of photoexcited carriers as we varied the compensation. At the lower values of  $N_d$ , from  $4.3 \times 10^{10}$  up to  $1.7 \times 10^{13} \text{ cm}^{-3}$ , the photo-Hall mobilities were identical to Hall mobilities in the region of overlap of the two measurements. This is good evidence that the photoexcited carrier population had a thermal distribution in these samples, at least in the overlap region. Figure 6 shows the Hall and photo-Hall mobility from 3 to 100 K. For samples with higher donor concentrations, there is a marked increase in mobility as the population of carriers shifts from thermal to optical excitation. This discontinuity was seen for all heavily compensated samples. A few relatively pure samples showed discontinuities in this same region, but it is believed that the cause of this behavior was non-uniformity in the impurity distribution. For this reason, we have not included these samples in this presentation.

A complete description of the lifetime measurements will be given in Paper III of this series.<sup>21</sup> We will use the measured result of the recombination cross section for this presentation. The cross section is defined in the usual sense:  $\sigma = (N_d \tau \langle v \rangle)^{-1}$ , where we have assumed that  $p \ll N_d$ , the density of compensation, and where  $\tau$  and  $\langle v \rangle$  are the carrier lifetime and average thermal hole velocity, respectively. This equation is obviously only valid in the range where the carriers are in thermal equilibrium with the lattice. The cross section was measured for samples 143.13, 145.1, and 146.1, and was found to be  $2.5 \times 10^{-12} (T/20)^{-n} \text{ cm}^2$ , where  $n$  varies from 1.6 to 1.0 for compensation between  $4.3 \times 10^{10}$  and  $2.5 \times 10^{12} \text{ cm}^{-3}$ .

#### IV. COMPARISON OF EXPERIMENT WITH THEORY

The experimental results indicate that photoexcited carriers have higher mobilities than thermally excited carriers when  $N_d$  is greater than about  $5 \times 10^{13} \text{ cm}^{-3}$ . This was seen qualitatively in Fig. 6. In order to estimate the carrier energy from the mobility, a series of calculated mobilities were graphed as a function of temperature, with an assumed carrier energy. We used the  $\delta$ -function distribution to define the carrier energy. This was then compared directly with the measured mobility, as illustrated in Fig. 7. The parameters used to calculate the mobility are:  $N_a$ , copper concentration per cubic centimeter;  $N_d$ , donor concentration per cubic centimeter;  $p$ , carrier concentration per cubic centimeter;  $A$ , correction factor multiplying the neutral-impurity-scattering time, to account for the nonhydrogenic nature of the copper impurity; and  $G$ , geometrical error factor multiplying the calculated mobility, to account for the error in measuring sample dimensions. These

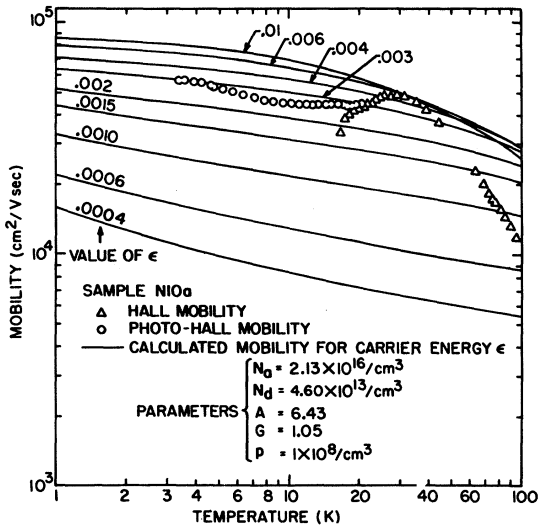


FIG. 7. Hall and photo-Hall mobility of sample N10a, compared with the mobility calculated for a  $\delta$ -function distribution of carrier energy  $\epsilon$ .

parameters were determined by computer fitting the Hall-mobility data for the samples, under thermal excitation of the carriers.<sup>8</sup> Figure 8 shows the photoexcited-carrier energy determined at four temperatures, as a function of the compensation density. At the lowest values of  $N_d$ , the energy is quite close to  $\frac{3}{2}kT$ , and rises to about 15 meV as the compensation reaches  $10^{15} \text{ cm}^{-3}$ . There is also a notable loss of any temperature dependence of the photocarrier energy for  $N_d$  greater than  $10^{13} \text{ cm}^{-3}$ .

Two remarks are in order on these calculations. The ionized-impurity-scattering formula is inappropriate at low temperatures for the heavily compensated samples, when the distribution is thermally generated.<sup>22,23</sup> This is because under these conditions  $|\vec{k}a|$  is not much greater than unity as

required by the Born approximation. However, the photoexcited carriers in such samples are not in thermal equilibrium and consequently have momentum values large enough to recover the validity of this approximation. For a typical case, sample N5a has a value of  $|\vec{k}a| = 6$ , with the conservative estimate of a 30-K effective carrier temperature and using the most stringent case of the light-hole effective mass.

To show that no significant systematic error arose in the analysis, we have evaluated the effective energy at 20 and 30 K using the Hall-mobility values. Results of this analysis are listed in Table I. No variation comparable to that found for the photo-Hall mobility is evident. This indicates that the  $\delta$ -function analysis did not show any unexpected bias as the scattering mechanism changed from predominantly lattice to predominantly ionized-impurity scattering.<sup>9,23</sup>

As can be seen in Fig. 8, the effective carrier energy begins to deviate from  $\frac{3}{2}kT$  at compensations between  $10^{12}$  and  $10^{13} \text{ cm}^{-3}$  for a temperature of 4 K. For temperatures of about 15 K, the increase in effective energy occurs for compensations slightly above  $10^{13} \text{ cm}^{-3}$ . Before comparing this conclusion with theory, a few remarks are in order on the carrier-injection process.

Photoionization of neutral-copper impurities requires a minimum photon energy of 42.86 meV. This is much less than the average photon energy from a 300-K source, which is on the order of 100 meV. Since the excess energy on the average is about 60 meV, the carrier will typically emit one or more optical phonons (37 meV), until the carrier energy is less than the optical-phonon energy. Optical-phonon emission takes place in about  $10^{-12} \text{ sec}$ ,<sup>24</sup> so that after a very short time the carriers will all have energies less than 37 meV. The consequences of this fact are that carriers injected with energies of  $\epsilon + 0.037n$ , where

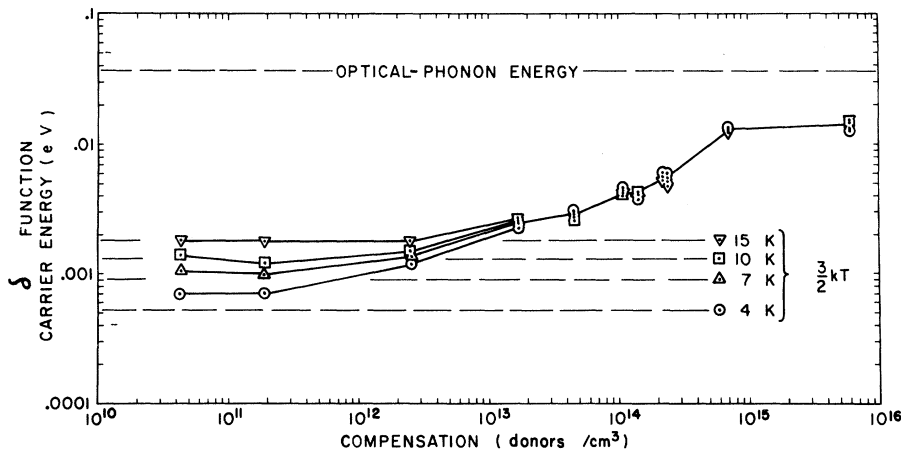


FIG. 8. Effective photo-carrier energy at four temperatures as a function of the compensation density. Energies are determined from evaluating the photo-Hall mobility as in Fig. 7.

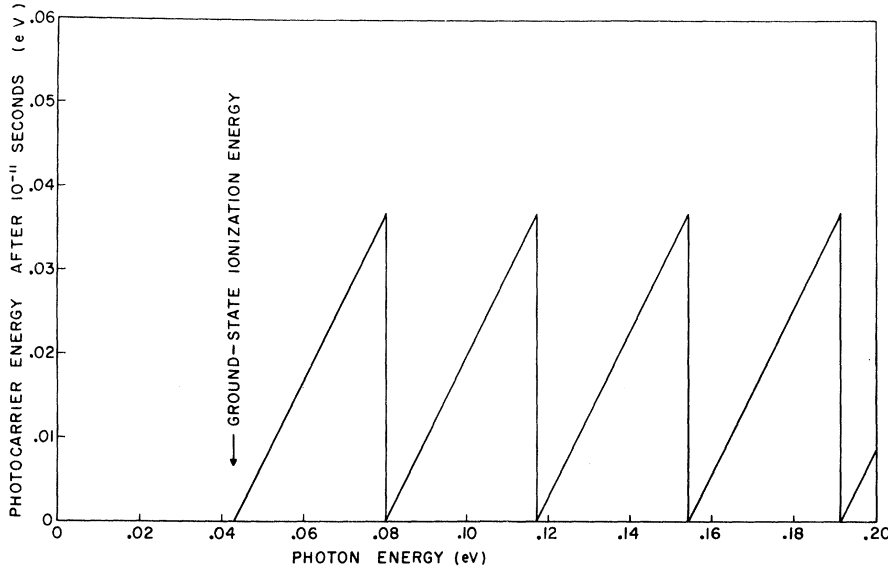


FIG. 9. The effective photo-excited carrier energy after about  $10^{-11}$  sec as a function of photon energy. Energy in excess of 0.037 eV is dissipated via optical-phonon emission in less than  $10^{-11}$  sec.

$n = 0, 1, 2, \dots$ , will all have energy  $\epsilon$  in about  $10^{-11}$  sec or less. Thus the carrier energy after about  $10^{-11}$  sec will be a repetitive ramp function of the photon energy. For clarity we illustrate this in Fig. 9. For a broadband source, such as 300-K background radiation, the average carrier energy will therefore be about 20 meV, at a short time after injection. Since the optical-phonon-emission process is very much faster than the carrier lifetime, even for quite heavily compensated samples, we can ignore the distribution of carriers with energies greater than 37 meV.

The thermalization time can be conveniently calculated by considering the rate of energy loss,  $d\epsilon/dt$ , via acoustic-phonon emission. The formula for the rate of energy loss is<sup>25-27</sup>

$$\frac{d\epsilon}{dt} = - \frac{E_1^2 m^* v^3}{\pi \rho \hbar^4}, \quad (7)$$

where  $E_1$  is the deformation potential constant,  $v$  is the carrier velocity, and  $\rho$  is the crystal density ( $\text{g}/\text{cm}^3$ ). For a parabolic band we find  $v^3 = (2\epsilon/m^*)^{3/2}$ . We wish to determine the time ( $\tau_{ac}$ ) required for a carrier injected with energy  $\epsilon_0$  to lose its excess energy. With the integration of time from 0 to  $\tau_{ac}$  and energy from  $\epsilon_0$  to  $\frac{3}{2}kT$  we find

$$\tau_{ac} = \frac{1.7 \times 10^{-10}}{E_1^2 m^{*3/2}} \left( \frac{1}{(\frac{3}{2}kT)^{1/2}} - \frac{1}{\epsilon_0^{1/2}} \right), \quad (8)$$

where  $E_1$ ,  $kT$ , and  $\epsilon_0$  are in electron volts. A plot of the thermalization time vs carrier-injection energy for the heavy-hole mass is shown in Fig. 10. A value of 10 eV was assumed for  $E_1$ .<sup>28</sup> At 4 K, thermalization of carriers injected with  $\epsilon_0$  equal to 20 meV requires about  $10^{-9}$  sec. The light-hole thermalization time is about 150 times longer using this same formula and the same value

for  $E_1$ . Consequently, thermalization of hot holes in the light-hole band will proceed through scattering into the heavy-hole band in the range of temperature above 1 K. This is because the interband scattering time for light holes is<sup>10</sup>

$$\tau_{12} = 1.83 \times 10^{-10} (T\epsilon^{1/2})^{-1} \text{ sec}, \quad (9)$$

where  $T$  is the absolute temperature, and  $\epsilon$  is in electron volts. For temperatures above 1 K, the light holes will scatter into the heavy-hole band faster than they thermalize within the light-hole band.

To compare this theory with experiment, we must compute the average carrier energy as a func-

TABLE I. Average carrier energy evaluated from Hall mobility using an assumed  $\delta$ -function distribution.

Sample	$N_d$ ( $\text{cm}^{-3}$ )	$\delta$ -function carrier energy (meV)	
		20 K	30 K
143.13	$4.3 \times 10^{10}$	3.0	4.8
145.1	$1.9 \times 10^{11}$	3.2	4.6
146.1	$2.5 \times 10^{12}$	5.5	6.0
N10b	$1.7 \times 10^{13}$	2.8	3.0
N10a	$4.6 \times 10^{13}$	2.8	5.5
N12h	$1.1 \times 10^{14}$	4.2	5.5
N5h	$1.4 \times 10^{14}$	3.6	5.0
N5g	$2.2 \times 10^{14}$	4.2	5.5
N5a	$2.4 \times 10^{14}$	3.8	5.5
N11i	$7.0 \times 10^{14}$	4.0	6.0
N5e	$6.0 \times 10^{15}$	...	7.0 <sup>a</sup>

<sup>a</sup>The very slight increase in the average energy with increasing  $N_d$  is explained by considering the change from lattice-dominated to ionized-impurity-dominated scattering. Because these mechanisms have different energy dependencies, the average over the thermal-energy distribution will peak at slightly different energies. This point has been made by Blatt (Ref. 23).

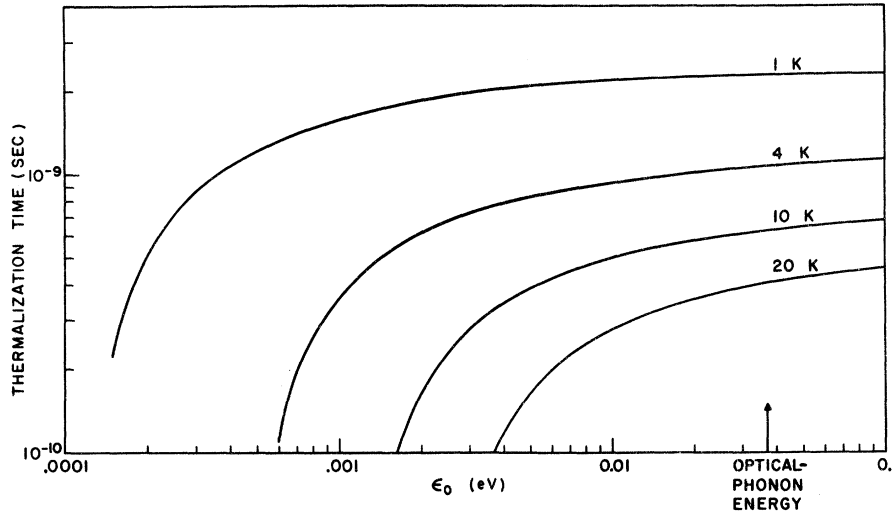


FIG. 10. Thermalization time for heavy holes in germanium calculated for carrier injection at energy  $\epsilon_0$  at four temperatures. Equations are given in the text.

tion of compensation. In the same spirit of our experimental analysis, we will omit averaging over the spread in carrier lifetimes, and concern ourselves only with average values. Let us first calculate the average carrier energy over its lifetime. The extremely short time spent at energies greater than 37 meV is ignored. The average carrier energy  $\bar{\epsilon}$  is then given by the following expression:

$$\bar{\epsilon} = \frac{\int_0^{\tau_{ac}} \epsilon(t) dt + \frac{3}{2} kT (\bar{\tau} - \tau_{ac})}{\bar{\tau}}, \quad \bar{\tau} \geq \tau_{ac}$$

$$= \frac{\int_0^{\bar{\tau}} \epsilon(t) dt}{\bar{\tau}}, \quad \bar{\tau} \leq \tau_{ac}, \quad (10)$$

where  $\bar{\tau}$  is the average carrier lifetime. The first term is the average carrier energy during the thermalization process. The second term is the average energy of the Boltzmann distribution. Each term is weighted by the amount of time a carrier spends at a particular energy. To evaluate the integral term we use

$$\epsilon(t) = [(E_1^2 m^{*5/2} / 1.7 \times 10^{-10}) t + \epsilon_0^{-1/2}]^{-2}. \quad (11)$$

With this, we find the average energy to be

$$\bar{\epsilon} = \frac{3}{2} kT \{1 + [(\epsilon_0 / \frac{3}{2} kT)^{1/2} - 1] (\tau_{ac} / \bar{\tau})\}, \quad \bar{\tau} \geq \tau_{ac}$$

$$= \epsilon_0 [1 + (E_1^2 m^{*5/2} / 1.7 \times 10^{-10}) \epsilon_0^{1/2} \bar{\tau}]^{-1}, \quad \bar{\tau} \leq \tau_{ac}. \quad (12)$$

In order to use this solution, we must now ask how the average carrier lifetime varies with carrier energy. For broadband radiation, the average effective input energy will be about 20 meV (see Fig. 9). Experimentally we have found a lifetime dependence of  $\epsilon^{1/2}$ , in agreement with other workers,<sup>6,29,30</sup> based on the electric field dependence of the lifetime. The average lifetime can then be written

$$\bar{\tau} = \frac{1}{\langle v \rangle \sigma N_d} \left( \frac{\epsilon}{\frac{3}{2} kT} \right)^{1/2}. \quad (13)$$

This expression must be averaged over the distribution of carrier energies. We ignore this and set  $\epsilon = \bar{\epsilon}$ , which is justified for the approximate accuracy we are seeking. It is now possible to construct a plot of  $\bar{\tau}$  as a function of  $N_d$ , the compensation density. We assume a value of  $\bar{\tau}$  and  $\epsilon_0$ , calculate  $\bar{\epsilon}$  from Eq. (12), and then find  $N_d$  from Eq. (13). Figure 11 shows the result for  $\epsilon_0 = 20$  meV, at both 4 and 15 K. This calculation is in remarkable agreement with the data obtained from the  $\delta$ -function mobility analysis. It is also interesting to plot  $\bar{\tau}$  as a function of  $N_d$  from this same calculation. This done in Fig. 12 and the numbers used in this calculation are listed in Table II for reference.

The model we have just developed gives good agreement with the change in the average photocarrier energy which was deduced from photo-Hall-mobility measurements. What we have assumed about the lifetime dependence on photocarrier energy does not give results completely consistent with our data. Let us compare the temperature dependence of the photocarrier concentration of sample N5g (Fig. 1) with Fig. 12. Experimentally we find no temperature dependence of the photocarrier concentration. Since the photocarrier concentration is proportional to the carrier lifetime, assuming the photoionization process is independent of temperature, our experiment indicates no temperature dependence of the lifetime. However, our calculation indicates a slope of  $T^{0.22}$ . This error is not thought to be serious, considering the approximations used in treating the problem. Extrapolation of the cross section is done without regard to the overlap of excited states, which is more pro-



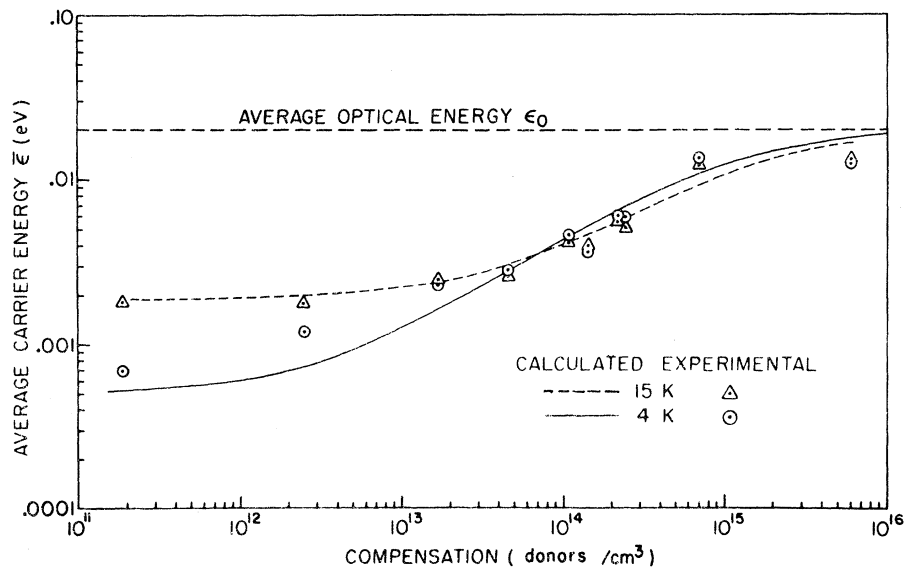


FIG. 11. Average photo-carrier energy calculated as a function of compensation. Experimental points are taken from an analysis of the photo-carrier mobilities as shown in Fig. 8.

nounced at high values of  $N_d$ . Considering the rather crude use of averages of the energy and lifetime in some cases, the experimental and theoretical agreement is considered good.

#### V. COMPARISON WITH OTHER EXPERIMENTS

Supporting evidence of carrier heating for compensation levels greater than about  $10^{13} \text{ cm}^{-3}$  is found in the results of oscillatory photoconductivity measurements. This effect was first reported in extrinsic InSb,<sup>31,32</sup> and has been observed in germanium doped with various impurities.<sup>33</sup> The theory for the electric field dependence of this effect has been discussed.<sup>34-36</sup> We consider here only the low-field limit, where the carrier gains no appreciable energy from the electric field. In this case, the oscillations in the photoconductive signal arise from the energy dependence of the mobility and carrier lifetime. In the case where the lifetime is sufficiently long, the injected carrier will thermalize, and its average energy will be independent of the injection energy. Therefore, there should be no oscillations in the photoconductive signal. However, when the lifetime becomes equal to or shorter than the thermalization time, the average energy of the carrier will be a function of its injection energy. Since the injection energy will follow the pattern of Fig. 9, the signal will oscillate in the same pattern. The oscillations will become more pronounced as the lifetime decreases with increasing compensation. Six copper-doped-germanium samples were studied by Besfamil'naya *et al.*,<sup>37</sup> and the relative depth of the oscillations was measured from the spectral response at 8 K. They reported a threshold of about  $6 \times 10^{13} \text{ cm}^{-3}$  compensation for the oscillatory effect, with the effect increasing rapidly for higher

compensation densities. Although their threshold occurs at higher compensations than ours, this may be due to differences in determining the compensation density.<sup>38</sup> Since the recombination cross sections used by Besfamil'naya *et al.* are also about an order of magnitude smaller than ours, it might be attributed, in part, to a difference in Hall analysis. Godik<sup>5</sup> has reported oscillations in copper-doped germanium at 10 K for a compensation level of  $1.6 \times 10^{13} \text{ cm}^{-3}$ . This is in agreement with our conclusion that the average carrier energy has begun to increase above  $\frac{3}{2}kT$  at this compensation density.

Quist<sup>39</sup> has measured the photoresponse of three copper-doped germanium samples for a range of  $N_d$  from  $10^{11}$  to  $10^{15} \text{ cm}^{-3}$ . The photoresponse showed the same variation as our measurements of

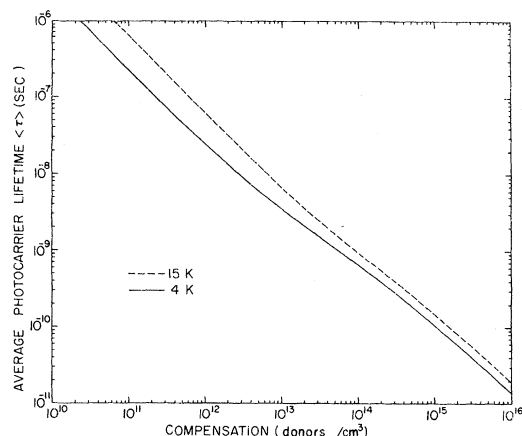


FIG. 12. Calculated average photocarrier lifetime as a function of compensation at 4 and 15 K, taking carrier thermalization into account.

TABLE II. Calculated average carrier energy and compensation density for a model based on acoustic-phonon thermalization of hot carriers and an energy-dependent carrier lifetime.

$\bar{\tau}$ (sec)	4 K		15 K	
	$\bar{\epsilon}$ (meV)	$N_d$ (cm <sup>-3</sup> )	$\bar{\epsilon}$ (meV)	$N_d$ (cm <sup>-3</sup> )
10 <sup>-6</sup>	0.52	2.3 × 10 <sup>10</sup>	1.94	6.4 × 10 <sup>10</sup>
3 × 10 <sup>-7</sup>	0.53	7.6 × 10 <sup>10</sup>	1.94	2.1 × 10 <sup>11</sup>
10 <sup>-7</sup>	0.54	2.3 × 10 <sup>11</sup>	1.94	6.4 × 10 <sup>11</sup>
3 × 10 <sup>-8</sup>	0.61	8.3 × 10 <sup>11</sup>	2.00	2.2 × 10 <sup>12</sup>
10 <sup>-8</sup>	0.78	2.8 × 10 <sup>12</sup>	2.14	6.7 × 10 <sup>12</sup>
3 × 10 <sup>-9</sup>	1.42	1.3 × 10 <sup>13</sup>	2.58	2.5 × 10 <sup>13</sup>
10 <sup>-9</sup>	3.22	5.7 × 10 <sup>13</sup>	3.88	9.1 × 10 <sup>13</sup>
3 × 10 <sup>-10</sup>	7.4	2.9 × 10 <sup>14</sup>	7.4	4.2 × 10 <sup>14</sup>
10 <sup>-10</sup>	12.8	1.1 × 10 <sup>15</sup>	12.8	1.7 × 10 <sup>15</sup>
3 × 10 <sup>-11</sup>	17	4.4 × 10 <sup>15</sup>	17	6.4 × 10 <sup>15</sup>
10 <sup>-11</sup>	19	1.4 × 10 <sup>16</sup>	19	2.0 × 10 <sup>16</sup>

Values assumed

4 K	15 K
$\tau_{ac} = 1 \times 10^{-9}$ sec	$\tau_{ac} = 4.5 \times 10^{-10}$ sec
$\frac{3}{2}kT = 5.17 \times 10^{-4}$ eV	$\frac{3}{2}kT = 1.94 \times 10^{-3}$ eV
$\langle v \rangle = 2.2 \times 10^8$ cm sec <sup>-1</sup>	$\langle v \rangle = 4.2 \times 10^6$ cm sec <sup>-1</sup>
$\sigma = 2.0 \times 10^{-11}$ cm <sup>2</sup>	$\sigma = 3.7 \times 10^{-12}$ cm <sup>2</sup>
$\epsilon_0 = 0.02$ eV	$\epsilon_0 = 0.02$ eV

carrier concentration as a function of temperature. Since the copper concentration was about  $7 \times 10^{15}$  cm<sup>-3</sup> for all three samples, we can expect the mobility to be relatively independent of temperature for the three samples measured by Quist. This is because the sample with lowest compensation should have a mobility dominated by neutral-impurity scattering below 20 K. The intermediate sample is similar to our sample N10b, while the heaviest compensation will produce very hot photocarriers, whose energy, and hence mobility, will be relatively temperature independent. Thus, the temperature dependence of his measured photo-

response should be proportional to the carrier lifetime. Although Quist did not feel that his data agreed with any of the usual theories of transport or recombination, our study shows that a consistent interpretation is possible by taking into account the carrier thermalization time.

A number of theoretical papers have dealt with the problems of hot photocarriers.<sup>30,40-42</sup> We have not tried to compare our experiments with any of these treatments, since none of them dealt with the important conditions for *p*-type germanium at low temperatures. The overwhelming importance of the role played by optical phonons cannot be neglected in constructing a theory of hot photoexcited carriers in *p*-type germanium. Under some conditions, such as temperatures below 1 K, it may be essential to include the degenerate nature of the valence band structure. Perhaps a calculation using the method of Barker and Hearn<sup>36</sup> would provide a convenient approach to this problem. Such a calculation, based on a Monte Carlo simulation of the injected-carrier life cycle, could also be extended into the region where the carrier lifetime approaches the time required for optical-phonon emission.

## VI. SUMMARY

The thermalization time of a hot photoexcited carrier in germanium is about 10<sup>-9</sup> sec at 4 K. This is in agreement with the assumption of energy loss via acoustic phonons. Interband scattering is very likely responsible for the thermalization of light holes, since this occurs much faster than the time required for a light hole to thermalize.

## ACKNOWLEDGMENTS

The technical assistance of T. Braggins, J. Keem, J. Roberts, and R. Strittmatter has been appreciated.

\*Work supported in part by the Air Force Avionics Laboratory.

<sup>1</sup>B. V. Rollin and J. M. Rowell, Proc. Phys. Soc. (London) **76**, 1001 (1960).

<sup>2</sup>R. S. Levitt and A. Honig, J. Phys. Chem. Solids **22**, 269 (1961).

<sup>3</sup>M. Loewenstein and A. Honig, Phys. Rev. **144**, 781 (1966).

<sup>4</sup>R. Maxwell and A. Honig, Phys. Rev. Letters **17**, 188 (1966); J. Phys. Soc. Japan Suppl. **21**, 319 (1966).

<sup>5</sup>E. E. Godik, Phys. Status Solidi **30**, K127 (1968).

<sup>6</sup>A. Yariv, C. Buczek, and G. S. Picus, in *Proceedings of the International Conference on the Physics of Semiconductors, Moscow, 1968* (Nauka, Leningrad, 1968), p. 500.

<sup>7</sup>H. Brooks, Phys. Rev. **83**, 879 (1951); in *Advances in Electronics and Electron Physics*, edited by L. Marton (Academic, New York, 1965), Vol. 7, p. 85.

<sup>8</sup>P. Norton and H. Levinstein, preceding paper, Phys.

Rev. B **6**, 470 (1972). The properties of all samples discussed in this paper are given in this reference.

<sup>9</sup>The average energy of a thermal distribution is  $\frac{3}{2}kT$ . For pure acoustic-phonon scattering, the  $\delta$ -function distribution will correspond to a carrier energy of  $1.7kT$ . For ionized-impurity scattering the value will be  $2.7kT$ . This error is much less than the range of energies found for hot-photocARRIER distributions.

<sup>10</sup>G. I. Bir, E. Normantas, and G. E. Pikus, Fiz. Tverd. Tela **4**, 1180 (1962) [Sov. Phys. Solid State **4**, 867 (1962)].

<sup>11</sup>M. Lax, Phys. Rev. **119**, 1502 (1960).

<sup>12</sup>H. H. Woodbury and W. W. Tyler, Phys. Rev. **105**, 84 (1957).

<sup>13</sup>E. O. Kane, J. Phys. Chem. Solids **1**, 82 (1956).

<sup>14</sup>A. C. Beer and R. K. Willardson, Phys. Rev. **110**, 1286 (1958).

<sup>15</sup>T. J. Bridges, T. Y. Chang, and P. K. Cheo, Appl. Phys. Letters **12**, 287 (1968).

<sup>16</sup>B. J. Rollin and J. P. Russell, Proc. Phys. Soc. (London) 81, 571 (1963).

<sup>17</sup>A. Miller and E. Abrahams, Phys. Rev. 120, 745 (1960).

<sup>18</sup>This definition is not meant to imply that the impurity-hopping conductivity can be subdivided into a carrier density and mobility. Only the quantity  $(n\mu)_i$  will be used, and not the separate components. It will, of course, have the same units as the product of these components.

<sup>19</sup>This is also good evidence that magnetic freeze-out was not important; see R. J. Sladek, J. Phys. Chem. Solids 5, 157 (1958). The argument here is that if the impurity wave functions were shrunk by the application of the magnetic field, then the impurity overlap would change, thus altering the hopping conductivity.

<sup>20</sup>J. R. Barker and C. J. Hearn, Phys. Letters 26A, 148 (1968).

<sup>21</sup>P. Norton and H. Levinstein, following paper, Phys. Rev. B 6, 489 (1972).

<sup>22</sup>N. Sclar, Phys. Rev. 104, 1548 (1956).

<sup>23</sup>F. J. Blatt, in *Solid State Physics*, edited by F. Seitz and D. Turnbull (Academic, New York, 1957), Vol. 4, p. 199.

<sup>24</sup>D. M. Brown and R. Bray, Phys. Rev. 127, 1593 (1962).

<sup>25</sup>F. Seitz, Phys. Rev. 76, 1376 (1949).

<sup>26</sup>E. M. Conwell, Phys. Rev. 135, A1138 (1964).

<sup>27</sup>A. Rose, RCA Rev. 27, 615 (1966).

<sup>28</sup>This value for  $E_1$  is only approximate, and may underestimate the thermalization time. Paige has used the hole mobility to calculate an effective value of 5.7 eV [E. S. G. Paige, in *Progress in Semiconductors*, edited by A. F. Gibson and R. E. Burgess (Wiley, New York, 1964) Vol. 8.] A discussion of the theory of the deformation potential has been given by G. L. Bir and G. E. Pikus, Fiz. Tverd. Tela 2, 2287 (1961) [Sov. Phys. Solid State 2, 2039 (1961)], for a complex band structure. If a value of 5.7 eV is used rather than 10 eV, the thermalization time will be about a factor of 3 longer. The theory of Rose (Ref. 27) gives a result for  $d\epsilon/dt$  that is a factor of

3 larger than the results of Seitz and Conwell (Refs. 25 and 26). Thus, our uncertainty in the choice of  $E_1$  is comparable to the difference in the two theoretical results.

<sup>29</sup>I. A. Chaikovskii and V. A. Kovarskii, Fiz. i Tekhn. Poluprov. 1, 1674 (1967) [Sov. Phys. Seimcond. 1, 1389 (1968)].

<sup>30</sup>A. P. Katsitadze, Z. S. Kachlishvili, and V. A. Morozova, Fiz. i Tekhn. Poluprov. 4, 1732 (1970) [Sov. Phys. Semicond. 4, 1486 (1971)].

<sup>31</sup>R. F. Blunt, Bull. Am. Phys. Soc. 3, 115 (1958).

<sup>32</sup>W. Engler, H. Levinstein, and C. R. Stannard, J. Phys. Chem. Solids 22, 249 (1961).

<sup>33</sup>C. Benoit a la Guillaume and J. Cernogora, J. Phys. Chem. Solids 24, 383 (1963).

<sup>34</sup>H. J. Stocker and H. Kaplan, Phys. Rev. 150, 619 (1966).

<sup>35</sup>B. L. Jones and P. R. Beaudet, Can. J. Phys. 45, 4091 (1967).

<sup>36</sup>J. R. Barker and C. J. Hearn, Phys. Letters 29A, 215 (1969).

<sup>37</sup>V. A. Besfamil'naya, I. A. Kurova, N. N. Ormont, and V. V. Ostroborodova, Zh. Eksperim. i Teor. Fiz. 48, 1588 (1965) [Sov. Phys. JETP 21, 1065 (1965)].

<sup>38</sup>The Hall data reported in Ref. 37 was analyzed using the degeneracy factor of 2, which is in disagreement with our analysis for copper-doped germanium (Ref. 8). A graphical analysis, in the freeze-out temperature region, indicates that the product of degeneracy times  $N_d$  should be equal to a constant, for  $N_a \gg N_d$ . Therefore, if a degeneracy of 2 is used instead of 4, this analysis will give twice the value of  $N_d$ .

<sup>39</sup>T. M. Quist, Proc. IEEE 56, 1212 (1968).

<sup>40</sup>C. J. Hearn, Proc. Phys. Soc. (London) 88, 407 (1966).

<sup>41</sup>V. N. Abakumov, R. I. Lyagushchenko, and I. N. Yassievich, Fiz. Tverd. Tela 10, 2920 (1968) [Sov. Phys. Solid State 10, 2309 (1969)].

<sup>42</sup>Y. P. Ladyzhinskii, Fiz. Tverd. Tela 11, 2282 (1969) [Sov. Phys. Solid State 11, 1842 (1970)].